

Partial turbulence simulation and aerodynamic pressures validation for an open-jet testing facility

Tuan-Chun Fu^{1a}, Arindam Gan Chowdhury^{2*}, Girma Bitsuamlak^{3b} and Thomas Baheru^{4c}

¹Department of Civil and Environmental Engineering, Florida International University,
10555 West Flagler St., Miami, FL, 33174, USA

²Department of Civil and Environmental Engineering, International Hurricane Research Center,
Florida International University, 10555 West Flagler St., Miami, FL, 33174, USA

³Department of Civil and Environmental Engineering, The University of Western Ontario, London, ON, Canada

⁴Department of Civil and Environmental Engineering, Florida International University,
10555 West Flagler St., Miami, FL, 33174, USA

(Received July 22, 2013, Revised January 23, 2014, Accepted February 22, 2014)

Abstract. This paper describes partial turbulence simulation and validation of the aerodynamic pressures on building models for an open-jet small-scale 12-Fan Wall of Wind (WOW) facility against their counterparts in a boundary-layer wind tunnel. The wind characteristics pertained to the Atmospheric Boundary Layer (ABL) mean wind speed profile and turbulent fluctuations simulated in the facility. Both in the wind tunnel and the small-scale 12-Fan WOW these wind characteristics were produced by using spires and roughness elements. It is emphasized in the paper that proper spectral density parameterization is required to simulate turbulent fluctuations correctly. Partial turbulence considering only high frequency part of the turbulent fluctuations spectrum was simulated in the small-scale 12-Fan WOW. For the validation of aerodynamic pressures a series of tests were conducted in both wind tunnel and the small-scale 12-fan WOW facilities on low-rise buildings including two gable roof and two hip roof buildings with two different slopes. Testing was performed to investigate the mean and peak pressure coefficients at various locations on the roofs including near the corners, edges, ridge and hip lines. The pressure coefficients comparisons showed that open-jet testing facility flows with partial simulations of ABL spectrum are capable of inducing pressures on low-rise buildings that reasonably agree with their boundary-layer wind tunnel counterparts.

Keywords: wall of wind; low-rise building; spectrum; roof; partial turbulence; pressure coefficient

1. Introduction

Observations of damage have shown that residential low-rise buildings are typically vulnerable to powerful wind storms. An improved understanding of wind effects on low-rise buildings is therefore needed. Simulations of wind effects on structures are primarily performed on small-scale

*Corresponding author, Dr., E-mail: chowdhur@fiu.edu

^a Dr., E-mail: tfu001@fiu.edu

^b Associate Professor, E-mail: gbitsuam@uwo.ca

^c Doctoral Graduate Assistant, E-mail: tbahe001@fiu.edu

(say, 1:100) building models, in wind tunnels that simulate atmospheric boundary layer (ABL) flows. However, there are some scaling issues while using boundary layer wind tunnel facilities, primarily constructed for high rise buildings, to study low-rise buildings. Kozmar (2010) found that flows with integral turbulence scales typically used for testing high-rise structures were inadequate for testing low-rise buildings. Nevertheless, wind tunnel studies remains industry wide accepted tools and test results so obtained are the main source for building code specifications on wind pressures.

With a view to testing of low-rise buildings at large scales for high resolution wind pressure measurements, testing of actual material characteristics, and coupled wind and wind driven rain tests, a large-scale 6-Fan Wall of Wind (WOW) open-jet wind engineering test facility (Fig. 1) was developed at Florida International University (FIU) (Huang *et al.* 2009).

The 6-fan WOW was used for performing tests on low-rise buildings subjected to strong winds (Aly *et al.* 2012, Bitsuamlak *et al.* 2009, Gan Chowdhury *et al.* 2009, Gan Chowdhury *et al.* 2010, Simiu *et al.* 2011, Tecele *et al.* 2013). However, the 6-Fan WOW facility was not capable of performing tests in flow speeds associated with higher category hurricanes (Leatherman *et al.* 2007). A more advanced large-scale 12-Fan WOW (Fig. 2), capable of producing wind velocities associated with Category 5 hurricanes was constructed at FIU and opened in 2012. Each fan has a maximum flow rate of 113.3 cubic meter/second (240,000 cubic foot/minute (cfm)) with a total pressure head of 3736 Pa (15 in. H₂O).

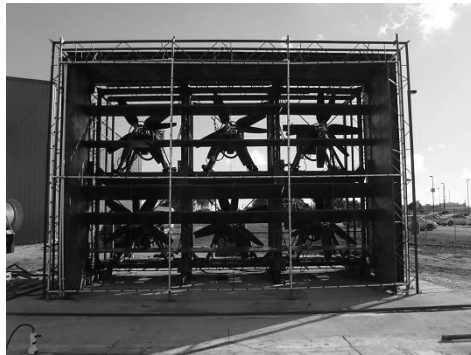


Fig. 1 6-Fan WOW at FIU



Fig. 2 Large-Scale 12-Fan WOW

The power rating of each motor driving the fan is 522 kilowatt (700hp). The fan speeds are controlled by variable frequency drives (VFD). The 12 fans are mounted on a steel frame and a contraction section boosts the mean wind speed up to 71.4 m/s (157mph). It is also necessary to assure that the 12-Fan WOW is capable of simulating reasonably well the main flow characteristics as of ABL winds including the mean wind profile and turbulence parameters. For this reason, flow management devices comprising of spires and roughness elements are to be designed to produce flows with characteristics close to those of natural winds and to those used in the boundary layer wind tunnels.

To save design time and resources, a cost effective small-scale 12-Fan replica (Fig. 3) with a model scale 1:15 was built with a view to developing the requisite flow management devices. In that replica, Aly *et al.* (2011) successfully reproduced natural wind characteristics for suburban exposure using active controls (i.e., running the fans with waveforms that can vary the fan speeds) and passive controls (using horizontal planks). A quasi-periodic waveform was used to control the fan speeds with a view to generating adequate turbulence intensity. In addition Aly *et al.* (2011) performed pressure measurements on models of the Silsoe building and the Texas Tech University experimental building, two structures for which measurements of pressures induced by natural wind were available.

The quasi-periodic waveform used by Huang *et al.* (2009) and Aly *et al.* (2011) in the small-scale 12-Fan WOW could not be employed in the large-scale 12-Fan WOW because its electrical components were not capable of generating rapid changes in the rotational velocity of the fans. Therefore, constant rotational speeds of the fans were used to simulate natural wind in the large-scale WOW. This paper describes the passive generation in the small-scale 12-fan WOW of flows simulating natural winds. The paper also reports results of tests in those flows of four typical low-rise buildings, and comparisons of those results with data obtained in wind tunnel tests. Comparisons between results obtained in the small-scale 12-Fan WOW and the wind tunnel are a useful indication of the capabilities of the WOW and are the initial steps toward the future validation of test results obtained in the large-scale 12-fan WOW.

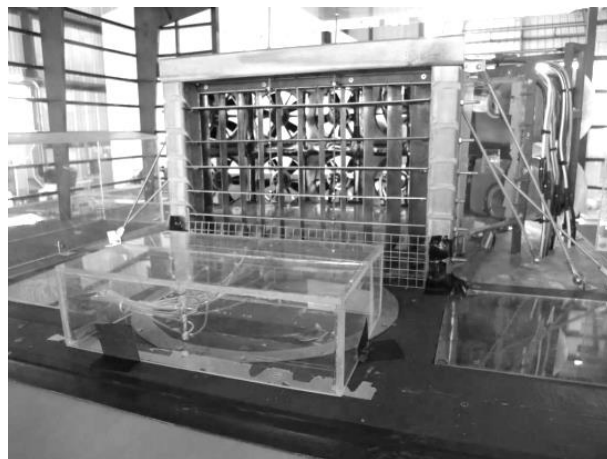


Fig. 3 1:15 Small-Scale 12-Fan WOW

2. Wind flow simulation and pressure measurements

Flow simulations in both the wind tunnel and the small-scale 12-Fan WOW were performed with a view to reproducing correctly target ABL flows and obtain reliable pressure data for low-rise buildings. In both facilities three spires as well as floor roughness elements (Fig. 4) were used to reproduce suburban wind profiles. Fig. 5 shows profiles generated in wind tunnel and the small-scale WOW, as well as the target prototype profile. The exponent of the power law describing the profiles is in all cases $\alpha \approx 0.25$. The mean wind velocities at reference height (mean roof height of building model) were approximately 8 m/s and 12.5 m/s for wind tunnel and small-scale WOW, respectively. However, the full longitudinal turbulence spectrum was reproduced in the wind tunnel, whereas in the small-scale WOW only partial longitudinal turbulence spectrum was simulated, as is shown in some detail subsequently in this paper.

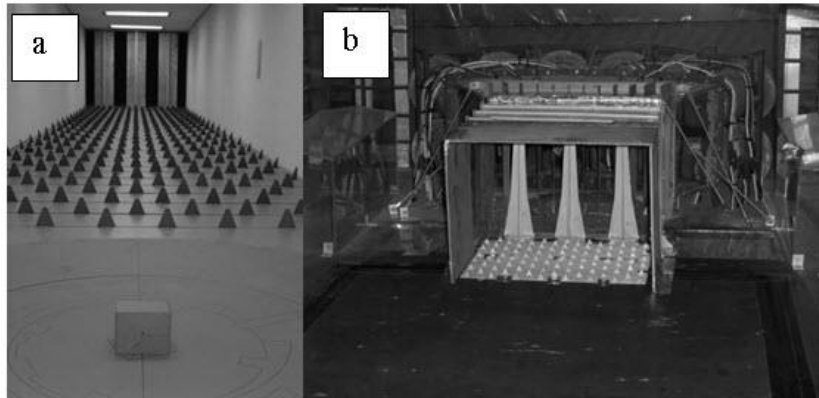


Fig. 4 (a) RWDI wind tunnel, (b) Small-Scale 12-Fan WOW with flow management devices

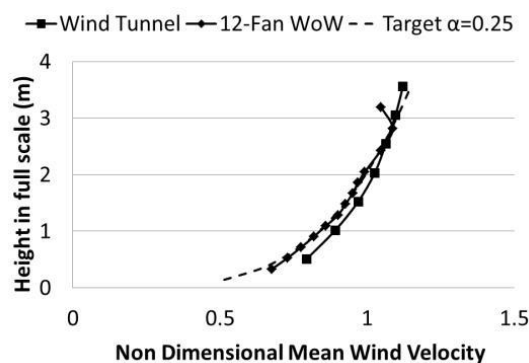


Fig. 5 ABL profile of wind tunnel, Small-Scale 12-Fan WOW, and Target ABL profile

2.1 WOW simulation of atmospheric boundary layer flow

2.1.1 Partial turbulence flow simulation in WOW

Melbourne (1980) introduced the small scale turbulence parameter $S = [nS_u(n)/\sigma_u^2](\sigma_u/U)^2 \times 10^6$ evaluated at frequency $n = 10U/L_B$ where $S_u(n)$ is the spectral density of the u -velocity component, σ_u is the RMS (root-mean-square) of the velocity component u , n is the frequency, and U is the mean wind velocity. The small scale or high frequency turbulence needs careful consideration for proper simulation of aerodynamic effects on low-rise structures. The isotropy of the turbulence structure is expected to occur in the so-called inertial subrange. The inertial subrange does extend up to the dissipation range, but the eddies with the highest frequencies within the inertial subrange (i.e., with frequencies closest to the dissipation range) are typically not significant aerodynamically. Saathoff and Melbourne (1997) investigated the effects of free-stream turbulence on surface pressure fluctuations near leading edges of sharp-edged bluff bodies. This experimental study showed that peak pressure fluctuations occur when free-stream perturbations cause the separated shear layer to roll-up near the leading edge. Tieleman (2003) pointed out that in order to conduct correct wind tunnel simulation for fluctuating pressures on a low-rise structure, it is necessary to duplicate the small scale turbulence at the height where the pressures are being measured. The small scale turbulence parameter, S , is appropriately based on the content of the turbulence in the incident flow with a wavelength comparable to the thickness of the separated shear layer. The latter is estimated for low-rise structures at 1:10 of their height. Richards *et al.* (2007) tested the well-known Silsoe building, and showed that wind tunnel flow for which high frequency turbulence components correctly reproduced their prototype counterparts produced mean and peak pressure coefficient (C_p) values that compared well with the respective values measured at full scale. Yamada and Katsuchi (2008) also proved that the flow field around a rectangular cylinder can be adequately simulated by adopting “partial simulation” considering only the high frequency turbulence. In their study, a Von-Karman type power spectral density model was considered to simulate the high-frequency part of the turbulence. More recently, Sangchuwang *et al.* (2013) observed the effects of “partial simulation” turbulence on sharp-edged bluff bodies. In their study, a new turbulence parameter, reduced turbulence intensity (I_r), was adopted to investigate the flow pattern around bluff bodies.

Based on the researches mentioned above it is apparent that pressures on buildings are significantly affected by small-scale turbulence (i.e., turbulence with scales considerably smaller than the building dimensions) because transport across the separation layers of flow particles with high momentum from outside the separation bubbles causes a change in the position of the flow reattachment points. This brings about changes in the pressure distribution over the surface of the body (Simiu 2011). Fluctuating aerodynamic effects are produced partly by turbulence in the oncoming flow, and partly by “signature turbulence,” that is, by turbulence due to flow separation from the body. The effects of “signature turbulence” tend to dominate at locations on the body where pressures are high (i.e., at “hot spots”).

The above statements illustrate that high frequency turbulence generation is important for the WOW simulation. This small scale turbulence affects some of the most critical aerodynamic features causing high suction due to (1) flow separation from sharp edges creating shear layers and separation bubbles, and (2) conical vortices originating at corners from cornering winds. Fig. 6 shows comparisons of full turbulence spectra for ABL flows (as simulated in the wind tunnel) and the small-scale WOW partial turbulence spectrum. It is seen that the high frequency portion of the WOW spectrum better matches its counterpart in the ABL spectra as compared to the low

frequency portion, which is much lower in the WOW. The missing low frequency portion represents the large scale turbulence that can be depicted by slowly moving gusts. As these large scale gusts were missing in the WOW simulation it was proposed by Yeo and Gan Chowdhury (2013) to compensate for the missing low-frequency content by increasing the mean wind speed U by ΔU .

The mean wind speed increment ΔU may be viewed as a flow fluctuation with zero frequency and perfect spatial coherence and, therefore, as a reasonable approximation of the missing low-frequency fluctuations in the spectrum (for more details see Fu *et al.* 2012, Yeo and Gan Chowdhury 2013). The authors' hypothesis is that because the frequencies of the bulk of the energy-containing motions are low (i.e., relatively close to zero), they are approximately equivalent in terms of their aerodynamic effects on the structure to an energy-containing motion with zero frequency (with infinite period), i.e., to an appropriately determined increment in the mean velocity. The experimental results presented in Section 3 of this paper are viewed as a validation of this hypothesis. As showed in Simiu *et al.* (2011), these assumptions are valid for small structures (such as single residential buildings and their components) for which, unlike for high-rise and large low-rise buildings, the coherence of the oncoming flow turbulence is close to unity over distances comparable to the dimensions of the structure. This approach is also hypothesized to be appropriate for experimentation on local aerodynamic effects, such as local pressures on roof components and claddings of limited sizes for which high coherence is expected over the component sizes. An example is measuring aerodynamic pressures on tiles, shingles, or roof pavers on building models large enough to accommodate those roof components.

To achieve a Reynolds number close to that in full scale, the WOW tests are conducted mostly at high wind speeds. Let U_{PS} represents the mean wind speed recorded during high speed aerodynamic testing in the WOW. The subscript PS stands for "partial spectrum," meaning that the low-frequency content of the WOW longitudinal velocity fluctuations spectrum is weaker than in the ABL. Thus the recorded mean wind speed U_{PS} for the WOW partial turbulence simulation, being 12.5 m/s at mean roof height for the current work, can be considered to be higher by ΔU than the mean wind speed of an ABL full turbulence flow for which the high frequency portion of the WOW and ABL spectra match. Let the mean wind speed in the ABL flow be denoted by U_{FS} at the mean roof height of the building. The subscript FS stands for "full spectrum," meaning that the ABL longitudinal velocity fluctuations spectrum has both the low- and high-frequency content inherent in typical models of ABL flows. Among other widely accepted representations, it is appropriate to represent non-dimensional spectra $nS(n)/U^2$, as functions of the Monin parameter nz/U , where n is the frequency and U is the mean wind speed at the reference height z (e.g., Richards *et al.* (2007), Banks (2012)). Based on an ABL flow reproduced in the wind tunnel, Fig. 6 shows dimensional full turbulence spectra obtained using two arbitrary mean wind speeds 10 m/s and 6 m/s at the reference height (taken as the mean roof height of a building model). It is apparent that the high frequency turbulence contents in the WOW flow is higher and lower than their full turbulence spectra counterparts obtained using 10 m/s and 6 m/s, respectively. Thus it is apparent that the high frequency portion of the WOW flow and the ABL flow will closely match only when a specific target mean wind speed is used to generate the ABL flow spectrum. The question is "What should be the target mean wind speed U_{FS} corresponding to the ABL flow that will allow the high frequency portion of the corresponding ABL spectrum to match the high frequency portion of the WOW spectrum corresponding to mean wind speed U_{PS} ?" The difference between U_{PS} and U_{FS} is essentially the mean wind speed increment ΔU required to compensate for the missing low frequency fluctuations, i.e.,

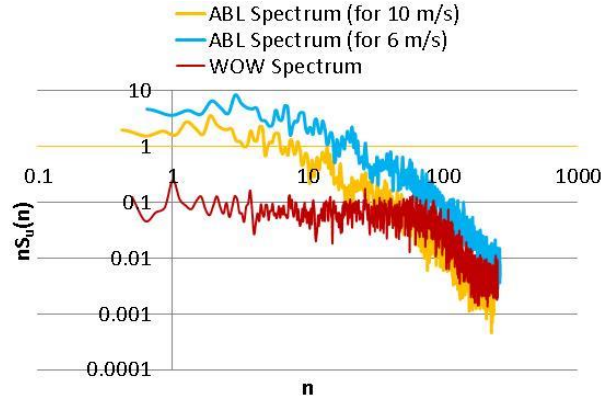


Fig. 6 Comparison of WOW partial turbulence spectrum with ABL full turbulence spectra obtained using two arbitrary mean wind speeds of 10 m/s and 6 m/s

$$\Delta U = U_{PS} - U_{FS} \quad (1)$$

It is shown in this paper that an adequate simulation of the ABL flow (with an estimated U_{FS}) can be achieved in the WOW by a flow with appropriate high-frequency content, thus simulating partial turbulence. Estimation of ΔU helps determine the missing low frequency content in the WOW flow. Knowing U_{PS} and estimating ΔU helps in the determination of U_{FS} , i.e., the target mean wind speed corresponding to which the high frequency portion of the ABL flow full spectrum will match its WOW counterpart. Given a model length scale λ_L , this U_{FS} can then be used to determine the velocity scale λ_v and the time scale λ_T . Based on the run time for an aerodynamic testing at WOW and the time scale λ_T , the corresponding duration at full scale can be estimated (e.g., 10 min, 20 min, etc.). Such equivalent full scale test duration information allows the estimation of statistics of peak pressures corresponding to any specified duration (say, 30 min or 1 hr.) based on the measured WOW pressure time histories. The estimation is performed using a statistical approach proposed by Sadek and Simiu (2002). Such WOW partial turbulence simulation technique will allow the flow to have correctly simulated high frequency turbulence components deemed of significant importance for peak pressure simulation by many researchers including Banks (2012), Richards *et al.* (2007), and Tieleman (2003). The aerodynamic pressures results for WOW shown in this paper are based on this partial turbulence simulation technique.

To estimate ΔU by using Eq. (1) it is necessary to determine the missing low turbulence content in the WOW partial turbulence spectrum. This requires, in turn, to determine the dimensional full turbulence spectrum whose high frequency turbulence portion matches its counterpart in the dimensional partial turbulence spectrum. Unless the mean speed U_{FS} in the expression for the target full spectrum is known, the dimensional full spectrum cannot be obtained from the corresponding non-dimensional full spectrum, since the latter depends upon U_{FS} through the reduced parameter $f=nz/U_{FS}(z)$, known as the Monin coordinate, (z = height above ground) or, if the von Karman spectrum is used, through the parameter $nL_u^x/U_{FS}(z)$ (L_u^x = integral length scale). Thus an iterative procedure is needed to obtain ΔU , as will be demonstrated in a following example.

For adequate simulation of the aerodynamic effects, it is required that the WOW flow with mean wind speed U_{PS} and deficient low-frequency fluctuations satisfy the relation

$$U_{PS}^{pk}(T) = U_{FS}^{pk}(T) \quad (2)$$

Where $U_{PS}^{pk}(T)$ = peak wind speed in the WOW partial turbulence flow simulation and $U_{FS}^{pk}(T)$ = peak wind speed in the full spectrum ABL flow counterpart. By definition the following relations hold

$$U_{PS}^{pk}(T) = U_{PS} + k_{u,PS}(T) \sigma_{u,PS} \quad (3a)$$

$$U_{FS}^{pk}(T) = U_{FS} + k_{u,FS}(T) \sigma_{u,FS} \quad (3b)$$

where $k_{u,PS}$ and $\sigma_{u,PS}$ = peak factor and RMS(root-mean-square) of longitudinal velocity fluctuations, respectively, for the WOW partial turbulence flow simulation, and $k_{u,FS}$ and $\sigma_{u,FS}$ = peak factor and RMS of longitudinal velocity fluctuations, respectively, for its full ABL flow counterpart. The WOW flows are considered stationary. Therefore the average wind speed for the test duration is considered to be the mean hourly wind speed. Thus T is taken as 3600 sec for calculating the peak factors used in the above equations. From Eqs. (1)-(3) it follows that

$$\Delta U = k_{u,FS} \sigma_{u,FS} - k_{u,PS} \sigma_{u,PS} \quad (4)$$

The expressions for the peak factors are

$$k_{u,FS}(T) = \sqrt{2 \ln(\gamma_{u,FS} T)} + \frac{0.577}{\sqrt{2 \ln(\gamma_{u,FS} T)}} \quad (5a)$$

$$k_{u,PS}(T) = \sqrt{2 \ln(\gamma_{u,PS} T)} + \frac{0.577}{\sqrt{2 \ln(\gamma_{u,PS} T)}} \quad (5b)$$

$$\gamma_{u,FS} = \left[\frac{\int_0^{n_c} n^2 S_{FS}(n) dn}{\int_0^{n_c} S_{FS}(n) dn} \right]^{1/2} \quad (5c)$$

$$\gamma_{u,PS} = \left[\frac{\int_0^{n_c} n^2 S_{PS}(n) dn}{\int_0^{n_c} S_{PS}(n) dn} \right]^{1/2} \quad (5d)$$

In Eqs. (5(c)) and (5(d)), n = dimensional frequency, n_c = cut-off frequency, $S_{FS}(n)$ = dimensional full spectrum (target spectrum), and $S_{PS}(n)$ = dimensional partial spectrum (i.e., spectrum with weak or negligible low-frequency content). Non-dimensional spectrum models (such as the Kaimal, Von Karman, or Davenport models) are generally used to represent the flow fluctuations for ABL flows. For WOW flow simulation, in lieu of ABL flow characteristics, flow characteristics measured in the wind tunnel may be used, provided that those characteristics match reasonably those of ABL flows. For this paper, suburban terrain ABL profiles were simulated in close circuit wind tunnel and open jet small-scale 12-fan WOW.

The description of the iterative procedure follows.

1. Based on Yeo and Chowdhury (2013), assume as a first approximation of U_{FS} and ΔU the values

$$U_{FS,1} = \frac{U_{PS}}{1.3} \quad (6a)$$

and

$$\Delta U_1 = U_{PS} - U_{FS,1} \quad (6b)$$

The mean wind speed U_{PS} is the mean wind speed used in the WOW testing. The latter is typically, though not necessarily, the largest speed obtainable in the WOW. For the small-scale 12-Fan WOW, $U_{PS} = 12.5$ m/sec (for $z_{ref} = 8.9$ cm, model mean roof height), therefore, assumed $U_{FS,1} = 12.5/1.3 = 9.6$ m/sec and $\Delta U_1 = 2.9$ m/sec.

2. Using the approximate value $U_{FS,1}$ and the specified prototype mean roof height z_{ref} , obtain, from the specified target non-dimensional full spectrum, the corresponding approximate dimensional full spectrum $S_{FS,1}(n)$ and the approximate RMS value $\sigma_{u,FS,1}$ corresponding to $S_{FS,1}(n)$. For this paper the target spectrum was the wind tunnel non-dimensional full spectrum based on the Von Karman model.
3. Substituting in Eq. (5(c)) the spectrum $S_{FS,1}(n)$ for $S_{FS}(n)$, obtain the approximation $\gamma_{u,FS,1}$ of $\gamma_{u,FS}$ and, using Eq. (5(a)), the corresponding approximation $k_{u,FS,1}(T)$ of $k_{u,FS}(T)$.
4. Using the WOW mean speed U_{PS} at the mean roof height z_{ref} obtain, from the non-dimensional partial spectrum measured in the WOW, the corresponding dimensional partial spectrum $S_{PS}(n)$ and the RMS value $\sigma_{u,PS}$.
5. From Eqs. (5(b)) and (5(d)), obtain the peak factor $k_{u,PS}(T)$.
6. Substituting in Eq. (4) the values obtained in steps 2, 3, 4 and 5, obtain the second approximation of ΔU_1 , denoted by ΔU_2 .

The procedure is repeated until the sequence ΔU_i ($i = 1, 2, \dots$) converges. For this particular case convergence was achieved after the fourth iteration with $U_{FS,4} = 8.5$ m/sec and $\Delta U_4 = 4.0$ m/sec. The dimensional target full spectrum and the WOW partial spectrum are shown in Figs. 7(a) and 7(b) for the first and the fourth iteration, respectively. It is to be noted that as the solution for ΔU converges the matching of the high frequency turbulence improves. Thus the target full spectrum mean wind speed $U_{FS,4} = 8.5$ m/sec results in a correct simulation of the high frequency turbulence components (see Figs. 7(b)-7(c), and the corresponding mean wind speed increment $\Delta U = 4.0$ m/sec can be viewed as a flow fluctuation compensating for the missing low-frequency fluctuations in the spectrum as stated earlier.

Fig. 8 shows the wind speed time histories where the peak wind speed in the WOW partial turbulence flow simulation matches closely the peak wind speed in the full spectrum ABL flow counterpart, satisfying Eq. (2).

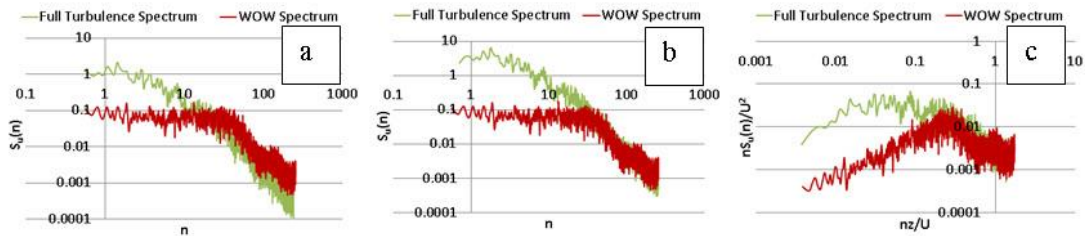


Fig. 7 Target full turbulence spectrum and WOW partial simulation spectrum (a) Dimensional spectra comparison at the beginning of iteration, (b) Dimensional spectra comparison at the end of iteration, (c) Non-dimensional spectra comparison at the end of iteration

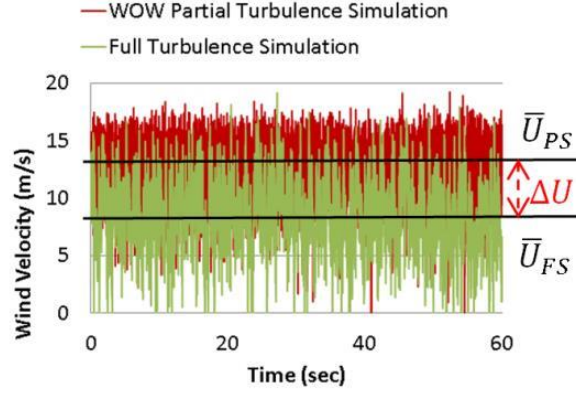


Fig. 8 Wind velocity time histories for WOW partial turbulence flow and ABL full turbulence flow

2.1.2 Reduced turbulence intensity

Irwin *et al.* (2008) stated that since past studies had discovered that small scale turbulence influences flow fields and aerodynamic parameters, therefore it is reasonable to match the power spectrum of turbulence only at high frequencies. For such partial turbulence simulation the turbulence intensity will have to be lower than that for the ABL flow containing the low frequency fluctuations. Katsuchi and Yamada (2011) and Sangchuwang *et al.* (2013) applied Irwin's approach to create new parameter "reduced turbulence intensity" combining turbulence intensity and turbulence scale together. Using the von Karman power spectral density model, the reduced turbulence intensity for partial turbulence simulation can be obtained from the equation

$$\left[\frac{I_u}{(L_u^x/D)^{1/3}} \right]_{PS} = \left[\frac{I_u}{(L_u^x/D)^{1/3}} \right]_{FS} \quad (7)$$

where I_u is the longitudinal turbulence intensity, L_u^x is the integral length scale, and D is the representative length. Thus the reduced turbulence intensity for the partial turbulence simulation can be obtained from the equation

$$[I_u]_{PS} = \left[\frac{I_u}{(L_u^x/D)^{1/3}} \right]_{FS} [(L_u^x/D)^{1/3}]_{PS} \quad (8)$$

The wind tunnel full spectrum turbulence intensity and integral length scale measured at model mean roof height were 25% and 0.7 m, respectively. The integral length measured in WOW was 0.05 m at 8.9 cm mean roof height of model. Using these values $[I_u]_{PS}$ can be estimated as about 12%. This value of suggested reduced turbulence intensity is close to the WOW turbulence intensity of 15% showing the adequacy of the turbulence intensity reduction to better match the power spectrum of turbulence only at high frequencies.

2.1.3 Velocity and time scaling

The test duration was 60 sec for each run during the building models pressure testing using the

12-Fan WOW. For Miami, the 3-second gust wind speed corresponding to open terrain and at 10 m above the ground is assumed to be 79.5 m/sec (175 mph) (Mean Recurrence Interval (MRI) 700 years, Risk Category II buildings and other structures; see ASCE 7-10). The corresponding mean hourly wind speed over suburban terrain and at 10 m above the ground is 35.5 m/sec (78.2 mph). Using the power law exponent $\alpha \approx 0.25$, the corresponding wind speed is 25.5 m/sec at $z = 2.67$ m (prototype mean roof height). Thus the WOW velocity scale is $\lambda_v = 8.5/25.5 = 1:3$ ($U_{FS,4} = 8.5$ m/sec is used in the numerator as that is the target mean wind speed for the flow with full turbulence). The model length scale being $\lambda_L = 1:30$, the WOW time scale is obtained as $\lambda_T = 1:10$. Thus the 1 min test duration at WOW represented 10 min at full scale. The velocity scaling should be based on the mean hourly wind speed U_{FS} , rather than on the 3-s gust wind speed. The determination of the 3-s gust speeds in the WOW must be based on the time scale λ_T . The latter is required to obtain the number of data points needed for the estimation of the wind speed averaged over 3 s, denoted by U_{3s} (see Section 2.2.2). The test duration for each run in the wind tunnel was 36 sec. For the wind tunnel (simulating the full turbulence spectrum) the scales were $\lambda_L = 1:20$, $\lambda_v = 1:3.3$ (based on the mean hourly wind speed for the wind tunnel), and $\lambda_T = 1:6$, thus 36 sec test duration represented 3.6 min at full scale. These equivalent full scale durations were used for peak pressure estimates given in Section 2.2.2.

2.2 Pressure measurements

2.2.1 Tubing correction system and tap locations

Scanivalve pressure acquisition systems were used in both WOW and wind tunnel facilities to capture pressure time history data with a 512Hz sampling rate. After collecting the raw data from the Scanivalve pressure scanner, a transfer function designed for the tubing system was used to correct the raw data. This method was developed by Irwin et al. (1979). The same tubing system was used in the wind tunnel and the WOW. In this system, 1.22 m (4 ft) PVC tubes with 1.34 mm (0.053 in) diameter connected the Scanivalve with pressure taps installed on the roof. The transfer function was applied to the raw time history data to obtain corrected mean and minimum (peak suction) pressure coefficient C_p values at 16 pressure taps. The pressure taps were located near roof corners, edges, ridge and hip lines where high suction is anticipated. Roof pressures were investigated only as roofs are the most vulnerable elements of low buildings and are often damaged from high suction pressures induced during windstorms such as hurricanes.

2.2.2 Pressure coefficients

The mean C_p value calculations were obtained as follows

$$C_{p \text{ mean}} = \frac{p(t)_{\text{mean}}}{\frac{1}{2}\rho U_{\text{mean}}^2} \quad (9)$$

where $p(t)_{\text{mean}}$ denotes the mean pressure, ρ is the air density, and U_{mean} is the mean wind velocity at the reference height (for the WOW pressure coefficients $U_{\text{mean}} = U_{PS}$). Peak C_p coefficients were obtained by using the equation

$$C_{p \text{ peak}} = \frac{p(t)_{\text{peak}}}{\frac{1}{2}\rho U_{3s}^2} \quad (10)$$

where $p(t)_{\text{peak}}$ is the estimated peak pressure and U_{3s} is the peak 3-s gust at the reference height.

For the WOW the wind speed U_{3s} was obtained by using the time scale $\lambda_T = 1:10$, meaning that

$512 \times 3/10 = 154$ data points were required for its determination. For the wind tunnel U_{3s} was obtained by using the time scale $\lambda_T = 1:6$, that is, $512 \times 3/6 = 256$ data points were required. The peak value of U_{3s} was obtained in both cases by performing moving averages.

To estimate the peak pressures with 5% probability of exceedance the Sadek and Simiu (2002) method was used. This method uses the entire time history, and the estimated values it obtains are more stable than observed peaks, which vary from observation to observation. A 10 min full-scale equivalent testing duration was adopted to allow meaningful peak pressure coefficient comparisons. As mentioned earlier, based on time scaling the 1 min test duration at WOW represented 10 min at full scale and the 36 sec test duration in the wind tunnel represented 3.6 min at full scale. In using the Sadek and Simiu (2002) method duration ratios $K=3$ and $K=1$ were applied to the time history data obtained in the wind tunnel and WOW, respectively, to obtain peak pressures for a 10 min full-scale equivalent duration.

3. Comparison of roof C_p Values obtained in the wind tunnel and the small-scale WOW

3.1 Low-rise building model testing

For the validation of aerodynamic pressures obtained using the WOW a series of tests were conducted in both wind tunnel and the small-scale 12-fan WOW facilities on low-rise buildings with various roof types and slopes including two gable roofs (slopes: 5:12, 7:12) and two hip roofs (slopes: 3:12, 5:12). The mean roof height of each building model at WOW was approximately 8.9 cm (i.e., 2.67 m in full scale). The gable and hip roofs had 2 cm overhangs (i.e., 0.6 m in full scale) on all sides. A typical small-scale WOW testing specimen with a gable roof is shown in Fig. 9.

The layout of the roof pressure taps for the models are shown in Figs. 10 and 11 for gable and hip roofs, respectively. Tests were performed for wind directions (i.e., angles of attack, or AOAs) $AOA = 0^\circ$ and a cornering wind angle of attack $AOA = 45^\circ$.

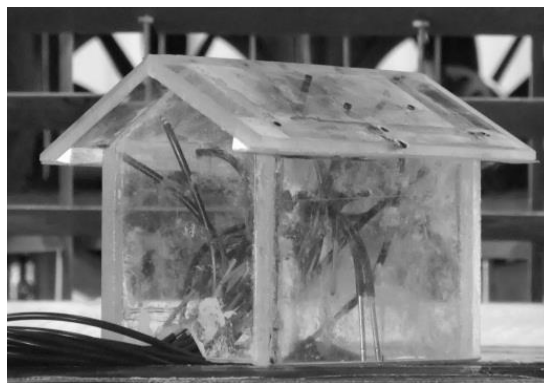


Fig. 9 A typical small-scale WOW testing specimen

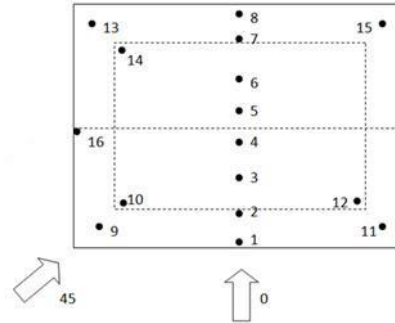


Fig. 10 Tap layout and wind angle of attack (AOA) for gable roofs (slope 5:12 and 7:12)

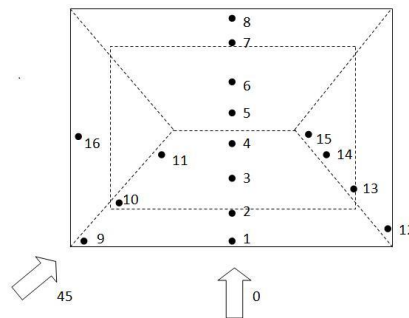


Fig. 11 Tap layout and wind angle of attack (AOA) for hip roof (slope 3:12 and 5:12)

Testing was performed to investigate the mean and peak pressure coefficients at the center lines, near ridge and hip lines, and corners of the buildings models. The mean and peak pressure coefficients (see Sec. 2.2.2) obtained using the WOW open-jet testing facility flows with partial simulation of ABL spectrum were compared with their boundary-layer wind tunnel counterparts obtained using flows simulating full ABL spectrum. The test results for each roof type are discussed in the following sections.

3.2 Gable roof buildings test results

Figs. 12 and 13 show the comparative results for the gable roof model with roof slope 7:12. Overall, the trend of the mean and peak pressure coefficients obtained in the two facilities (wind tunnel, W.T. and Wall of Wind, WOW) compared well with each other. The mean values match well for most taps including the edge and corner pressure taps for both wind angles of attack except for tap 1 for $AOA = 0^\circ$. For the critical taps under high suction pressures, the maximum difference among the C_p values obtained in the two facilities was below 6%. For $AOA = 0^\circ$ the peak pressure coefficients for all the tap locations, including the leading edge tap 1 and the windward and leeward corner taps 9 to 15, show good agreement between the WOW and wind tunnel. The highest (in magnitude) peak suction coefficient was obtained for the leeward overhang

tap 8. For $AOA = 45^\circ$, the peak pressure coefficients show reasonably good agreement except for the leeward corner taps 13 and 14 for which weaker (by approximately 20%) suction was shown for WOW testing. It is to be noted that the values of the highest peak suction coefficients in most cases showed good agreement, for example, leeward overhang tap 8 coefficients for $AOA = 0^\circ$ being -1.5 for both WOW and wind tunnel; tap 5 coefficients for $AOA = 45^\circ$ being -1.95 and -2.1 for WOW and wind tunnel, respectively, showing the effect of flow separation at the ridge for a steep sloped gable roof (lower suction coefficient of -0.5 was noted for tap 4 near the windward side of the ridge); gable end tap 16 (near the ridge) coefficients for $AOA = 45^\circ$ being close to -2.2 for both facilities.

Figs. 14 and 15 show the comparative results for the gable roof model with roof slope 5:12. The mean pressure coefficients obtained in the two facilities compared well with each other including those for the edge and corner pressure taps for $AOA = 0^\circ$; the difference for the highest suction at tap 8 was less than 10%. The peak pressure coefficients also show similar trends for both facilities. The peak values agree well for $AOA = 0^\circ$ for most taps except for the leading edge taps 1 and 2 for which the WOW peak pressure coefficients were higher in magnitude than those obtained from the wind tunnel. The mean and peak pressure coefficients agree well for $AOA = 45^\circ$ for most taps except for the leeward taps 6 and 16 for which the WOW showed a weaker suction. For $AOA = 45^\circ$, similar to the 7:12 roof model, the 5:12 roof model showed high suctions for tap 16 near the gable end ridge and tap 5 immediately downwind of the ridge.

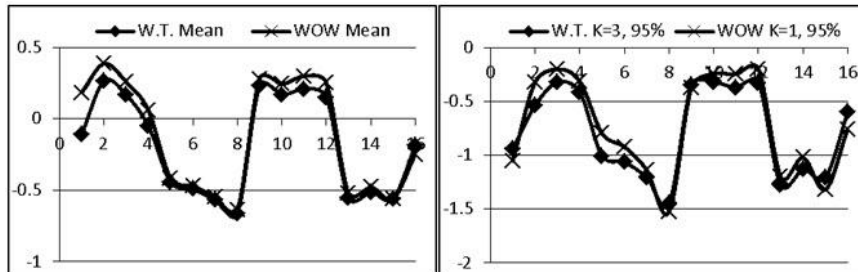


Fig. 12 Gable roof 7:12 mean (left) and peak (right) C_p for $AOA = 0^\circ$

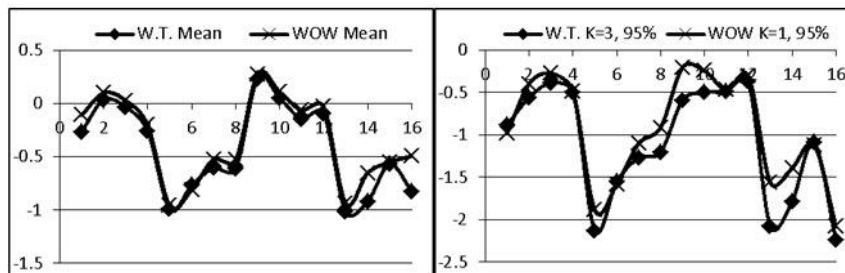


Fig. 13 Gable roof 7:12 mean (left) and peak (right) C_p for $AOA = 45^\circ$

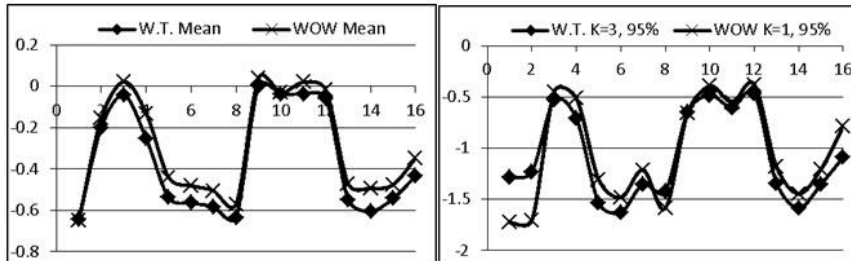


Fig. 14 Gable roof 5:12 mean (left) and peak (right) Cp for AOA = 0°

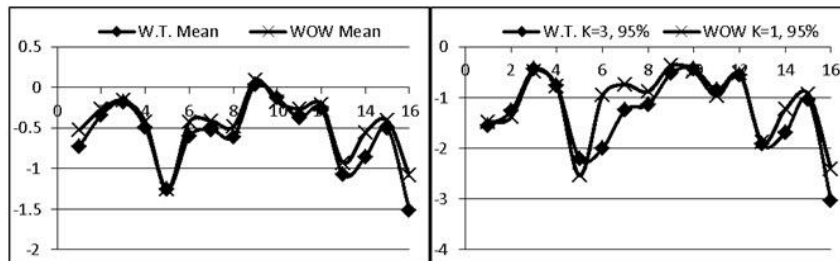


Fig. 15 Gable roof 5:12 mean (left) and peak (right) Cp for AOA = 45°

3.3 Hip roof buildings test results

Figs.16 and 17 show the comparative results for the hip roof model with roof slope 5:12. The mean pressure coefficients show reasonable agreement for the two facilities for most taps; for AOA = 0° the difference for the highest suction at tap 13 was less than 10% and for AOA = 45° the difference for the highest suction at tap 5 was about 5%. The peak pressure coefficients show similar trends for both facilities. The peak values match well for most taps except for the leading edge tap 1 for which the WOW shows a stronger and weaker suction for AOA = 0° and AOA = 45°, respectively. The values of the highest peak suction coefficients among all taps showed good agreement. For tap 13 the coefficients obtained in both facilities were close to -3.1 and -3.0 for AOA = 0° and AOA = 45°, respectively (only a difference of 2% for tap 13 was observed between the results of two facilities). It is to be noted that tap 13 peak suction, occurring downwind of the sloped hip for the 5:12 hip roof, was as high as the worst peak suction for the 5:12 gable roof occurring near the gable endridge at tap 16. All the taps 12, 13, 14, and 15 downwind of the sloped hip showed high suctions for both AOAs for the 5:12 hip roof. This shows the vulnerability of roofing components near gable end ridge and downwind of sloped hip locations that can be subjected to high suctions during extreme wind events. Both the wind tunnel and the WOW produced comparable high suctions near the gable end ridge and sloped hip for the roof models tested.

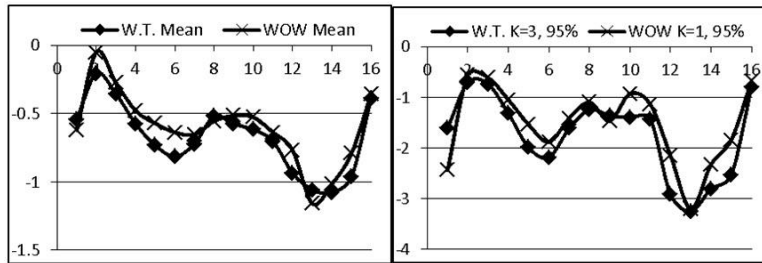


Fig. 16 Hip Roof 5:12 mean (left) and peak (right) Cp for AOA = 0°

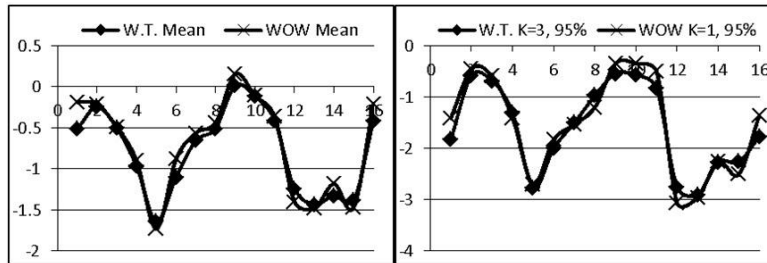


Fig. 17 Hip roof 5:12 mean (left) and peak (right) Cp for AOA= 45°

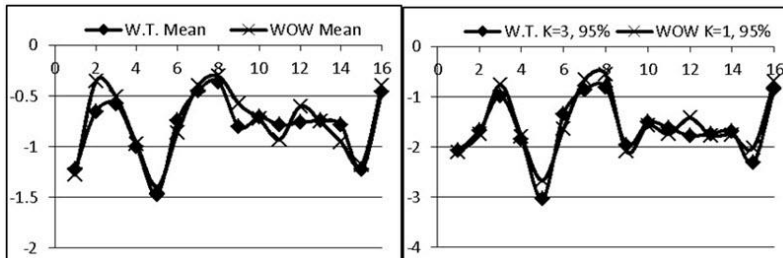


Fig. 18 Hip Roof 3:12 mean (left) and peak (right) Cp for AOA = 0°

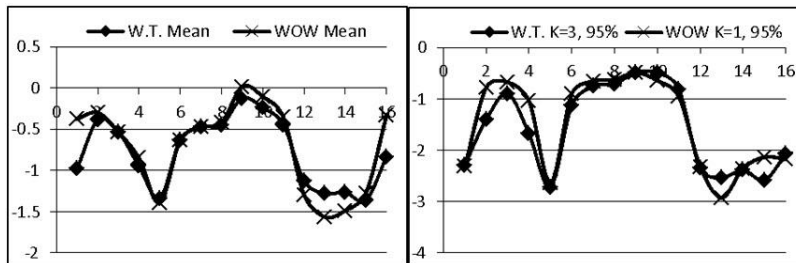


Fig. 19 Hip Roof 3:12 mean (left) and peak (right) Cp for AOA=45°

Figs. 18 and 19 show the comparative results for the hip roof model with roof slope 3:12. For $AOA = 0^\circ$ the mean and peak pressure coefficients obtained in the two facilities compared well with each other for the taps under higher suctions. For $AOA = 45^\circ$ the mean values match well for most taps except for taps 1, 13, and 14. However, for the same AOA the peak values match well for the taps with the highest suctions (taps 1, 5, 13). For tap 13, the WOW peak pressure coefficient was 15% higher than its wind tunnel counterpart. Similar to the 5:12 hip roof, the 3:12 hip roof showed highest peak suction coefficients occurring downwind of the sloped hip for $AOA = 45^\circ$ (taps 12, 13, 14, 15) and downwind of the ridge for both AOAs (for tap 5 the difference was 3% between two facilities). Also, both facilities simulated the high suction effects at the leading edge of the low sloped 3:12 roof. The leading edge tap 1 peak pressure coefficients were about -2.1 and -2.3 for $AOA = 0^\circ$ and $AOA = 45^\circ$, respectively (only a difference of 1.3% was observed between the results of two facilities).

4. Conclusions

Both wind flow simulation and pressure field validation for the small-scale 12-Fan WOW were presented in this paper by comparing WOW flow characteristics and pressure values and their wind tunnel counterparts. A suburban exposure wind profile with a reduced longitudinal turbulence intensity was generated in the small-scale 12-fan WOW to better simulate the high frequency turbulence in the ABL flow. A partial turbulence spectrum simulation was achieved in the WOW to allow the flow to have correctly simulated small scale turbulence components deemed of significant importance for peak pressure simulation by many researchers. An iteration procedure was developed to estimate the incremental wind speed ΔU that can be viewed to compensate for the absence of the low-frequency content in the WOW flow. The ΔU obtained at the end of the iteration allows obtaining the mean wind speed U_{FS} for an equivalent ABL flow such that the high frequency turbulence in the WOW spectrum matches its full turbulence spectrum counterpart. The mean wind speed U_{FS} was used to obtain scaling parameters needed to convert the actual test duration in WOW to an equivalent full scale duration to facilitate the comparison of estimated peak pressures for the WOW simulation and the wind tunnel ABL flow simulation. Pressure measurements and comparison of mean and peak pressure coefficient estimates for the partial turbulence flow in WOW and full turbulence flow in the ABL wind tunnel showed that this partial turbulence approach was effective aerodynamically. For four gable and hip roof low rise building models it was shown that both the wind tunnel and the WOW produced comparable high suctions (high peak pressure coefficients) for critical locations near the (1) leading edge for low-slope roof (e.g., tap 1 for 3:12 hip roof for $AOA = 0^\circ$ and $AOA = 45^\circ$); (2) leeward edge (e.g., tap 8 for 7:12 and 5:12 gable roofs for $AOA = 0^\circ$), (3) gable end ridge (e.g., tap 16 for 7:12 and 5:12 gable roofs for $AOA = 45^\circ$), (4) downwind of ridge (e.g., tap 5 for all roofs for both AOAs), and (5) downwind of sloped hip (e.g., taps 12, 13, 14, 15 for hip roofs for both AOAs). The test results agree with the findings by Teclé *et al.* (2013) showing the presence of high suction at the ridge compared to the edge zones. Also, the results showed that similar high suction can occur near the gable end ridge (tap 16) for cornering wind and the downwind side of the sloped hip (tap 13) for both cornering wind and wind perpendicular to the eave. Thus the traditional practice of considering gable roofs to be more vulnerable than hip roofs may not be applicable to the design of roofing elements, especially those at the sloped hip locations. The findings from the current tests provide an explanation to why failures initiate mostly at these ridge and hip locations, as

observed in recent post damage assessments: “Aerial photos taken after Ike showed close to 90 percent of the homes near the coast toward the western part of Bolivar Peninsula had an extensive loss of hip and ridge shingles”: (IBHS 2009).

Acknowledgements

The project was funded by the National Science Foundation (NSF Award No. CMMI-0928740 and 1151003). The Wall of Wind instrumentation was supported by NSF MRI Award (No. CMMI-0923365). The authors would like to acknowledge the support from NSF, Sea Grant Programs, DOE, FL DEM, Renaissance Re, Roofing Alliance for Progress, and AIR Worldwide. We greatly appreciate the discussions with Dr. Emil Simiu and Dr. Peter Irwin. We also express our appreciation to RWDI USA LLC for their great support in performing the tests for this study.

References

- American Society of Civil Engineers (2010), *Minimum design loads for buildings and other structures*, ASCE Standard, ASCE/SEI 7-10, New York City.
- Aly, A.M., Bitsuamlak, G.T. and Chowdhury, A.G. (2012), “Full-scale aerodynamic testing of a loose concrete roof paver system”, *Eng. Struct.*, **44**, 260-270.
- Aly, A.M., Gan Chowdhury, A. and Bitsuamlak, G. (2011), “Wind profile management and blockage assessment of a new 12-Fan Wall of Wind facility at FIU”, *Wind Struct.*, **14**(4), 285-300.
- Banks, D. (2012), *Measuring peak wind loads on solar power assemblies*, CCP Wind Engineering, Colorado, USA.
- Bitsuamlak, G.T., Gan Chowdhury, A. and Sambare, D. (2009), “Application of a full-scale testing facility for assessing wind-driven-rain intrusion”, *Build. Environ.*, **44**(12), 2430-2441.
- Fu, T.C., Aly, A.M., Gan Chowdhury, A., Bitsuamlak, G., Yeo, D. and Simiu, E. (2012), “A proposed technique for determining aerodynamic pressure on residential homes”, *Wind Struct.*, **15**(1), 27-41.
- Gan Chowdhury, A., Simiu, E. and Leatherman, S.P. (2009), “Destructive testing under simulated hurricane effects to promote hazard mitigation”, *Nat. Hazard. Rev.*, **10**(1), 1-10.
- Gan Chowdhury, A., Bitsuamlak, G. and Simiu, E. (2010), “Aerodynamic, hydro-aerodynamic, and destructive testing”, *J. ICE Struct. Build.*, **163**(2), 137-147.
- Huang, P., Gan Chowdhury, A., Bitsuamlak, G. and Liu, R. (2009), “Development of devices and methods for simulation of hurricane winds in a full-scale testing facility”, *Wind Struct.*, **12**(2), 151-177.
- Institute for Business & Home Safety (IBHS) (2009), “Hurricane Ike – Nature’s Force vs. Structural Strength”.
- Irwin, P., Cooper, K. and Girard, R. (1979), “Correction of distortion effects caused by tubing systems in measurements of fluctuating pressures”, *J. Wind Eng. Ind. Aerod.*, **5**(1-2), 93-107.
- Irwin, P. (2008), “Bluff body aerodynamics in wind engineering”, *J. Wind Eng. Ind. Aerod.*, **96**, 701-712.
- Katsuchi, H. and Yamada, H. (2011), “Study on turbulence partial simulation for wind-tunnel testing of bridge deck”, *Proceedings of the ICWE 12*, Amsterdam, Netherlands.
- Kozmar, H. (2010), “Scale effects in wind tunnel modeling of an urban atmospheric boundary layer”, *Theor. Appl. Climatol.*, **100**, 153-162.
- Leatherman, S.P., Gan Chowdhury, A. and Robertson, C.J. (2007), “Wall of Wind full-scale destructive testing of coastal houses and hurricane damage mitigation”, *J. Coastal Res.*, **23**(5), 1211-1217.
- Melbourne, W.H. (1980), “Turbulence effects on maximum surface pressures – a mechanism and possibility of reduction”, *Wind Eng.*, **1**, 521-551.
- Richards, P.J., Hoxey, R.P., Connell, R.P. and Lander, D.P. (2007), “Wind-tunnel modelling of the Silsoe

- Cube”, *J. Wind Eng. Ind. Aerod.*, **95**, 1384-1399.
- Sangchuwong, P., Yamada, H. and Katsuchi, H. (2011), “Study on turbulence effects on flow patterns around rectangular cylinders”, *Proceedings of the BBAA 7*, Shanghai, China.
- Sangchuwang, P., Yamada, H. and Katsuchi, H. (2013), “Study on turbulence effects on flow fields around sharp-edged bluff bodies”, *J. Struct. Eng. - ASCE*, **59**, 627-636.
- Saathoff, P.J. and Melbourne, W.H. (1997), “Effects of free-stream turbulence on surface pressure fluctuation in a separation bubble”, *J. Fluid Mech.*, **337**, 1-24.
- Sadek, F. and Simiu, E. (2002), “Peak non-Gaussian wind effects for database-assisted low-rise building design,” *J. Eng. Mech. - ASCE*, **128**(5), 530-539.
- Simiu, E. (2011). *Design on buildings for wind*, 2nd Ed., Hoboken: Wiley.
- Simiu, E., Bitsuamlak, G., Gan Chowdhury, A., Li, R., Tecle, A. and Yeo, D.H. (2011), “Testing of residential homes under wind loads”, *Nat. Hazard. Rev.*, **12**(4), 166-170.
- Tecle, A., Bitsuamlak, G., Suksawang N., Gan Chowdhury, A. and Fuez, S. (2013), “Ridge and field tile aerodynamics for a low-rise building: a full-scale study”, *Wind Struct.*, **16**(4), 301-322.
- Tieleman, H.W. (2003), “Wind tunnel simulation of wind loading on low-rise structures: a review”, *J. Wind Eng. Ind. Aerod.*, **91**(12-15), 1627-1649.
- Yamada, H. and Katsuchi, H. (2008), “Wind-tunnel study on effects of small-scale turbulence on flow patterns around rectangular cylinder”, *Proceeding of the 4th International Colloquium on Bluff Bodies Aerodynamics & Applications*, Italy.
- Yeo, D. and Gan Chowdhury, A. (2013), “A simplified wind flow model for the estimation of aerodynamic effects on small structures”, *J. Eng. Mech. - ASCE*, **139**, 367-375.